Journal of the Brazilian Society of Mechanical Sciences and Engineering (2018) 40:73
https://doi.org/10.1007/s40430-018-0999-6

TECHNICAL PAPER

Numerical simulation for homogeneous–heterogeneous reactions in flow of Sisko fluid

Tasawar Hayat[1,2] · Ikram Ullah[1] · Ahmed Alsaedi[2] · Bashir Ahmad[2]

Received: 9 March 2017 / Accepted: 10 November 2017 / Published online: 23 January 2018

Abstract

Magnetohydrodynamic flow of Sisko liquid over a stretching surface is addressed. Stretching property of sheet is the main agent for fluid flow. Heat transfer is modelled by convective condition. Homogeneous–heterogeneous reactions are also attended. Ordinary differential systems are acquired by using proper transformations. The resulting non-linear system is solved via ND solve shooting technique. Graphs are interpreted to examine the behavior of sundry embedded parameters on temperature and concentration profiles. Also surface drag forces and heat transfer rate are inspected for the impact of numerous pertinent variables. It is revealed that increasing magnetic parameter diminishes the temperature profile. Further for higher values of homogeneous reaction parameter the surface concentration reduces. In addition the verification of present results is achieved by developing comparison with already existing work. The results are found in an excellent agreement.

Keywords Three-dimensional flow · Homogeneous–heterogeneous reactions · Sisko liquid · MHD · Convective conditions

Abbreviation

u, v, w	Velocity components
x, y, z	Space coordinates
T	Temperature
T_f	Convective liquid temperature
T_∞	Ambient fluid temperature
B_0	Uniform magnetic field strength
A_1, A_2	Chemical species
D_A, D_B	Diffusion species
c, d, a_0	Positive dimensional constants
a_1, b_1	Concentration of chemical species
a, b, n $(n > 0)$	Material parameters
k	Thermal conductivity
h_f	Convective heat transfer
ξ	Transformed coordinate
K_c, K_s	Rate constant
K_1	Measure of strength of homogeneous reaction
K_2	Measure of strength of heterogeneous reaction
θ	Dimensionless temperature
M	Magnetic parameter
Le	Lewis number
Pr	Prandtl number
β	Material parameter of Sisko liquid
s_c	Schmidt number
C_{fx}, C_{fy}	Surface drag coefficients
Re_a, Re_b	Local Reynolds numbers
Nu_x	Local Nusselt numbers
U_w, V_w	Surface stretching velocities
σ	Electrical conductivity
v	Kinematic viscosity
c_p	Specific heat at constant pressure
α	Ratio parameter
ρ	Density
μ	Dynamic viscosity
δ_1	Diffusion coefficient ratio
$\O$	Dimensionless concentration

Technical Editor: Cezar Negrao.

✉ Ikram Ullah
ikram020@yahoo.com

[1] Department of Mathematics, Quaid-I-Azam University 45320, Islamabad 44000, Pakistan

[2] NAAM Research Group, Faculty of Science, King Abdulaziz University, P. O. Box 80207, Jeddah 21589, Saudi Arabia

1 Introduction

The analysis regarding heat transfer phenomena towards stretched surface captured the attention of numerous investigators and scientists owing to its extensive demands in industrial and engineering processes. These applications includes wire drawing, crystal growing, brisk spray cooling, liquid films in condensation process, broadsheet manufacture, cooling of metallic sheet, construction of sticky tape, continuous modeling of metals, portrayal of plastic films, ice cooler in air-conditioning frameworks, glass blowing, etc. The quality of end product in industry highly depends upon both the stretching and cooling rate. Flow induced by stretching of sheet is initially explored by Crane [1]. Afterwards several attempts have been made on stretched flows and heat transported characteristics. Cortell [2] explored the aspects of viscous dissipation and thermal radiation over a stretched flow. Ibrahim et al. [3] studied MHD stretched flow of nanofluid. An exponentially stretched 3D flow with radiation aspects is examined by Mustafa et al. [4]. Electrical MHD nanoliquid flow with slip effects on a stretching sheet is documented by Hsiao [5]. The simultaneous aspect of melting heat transfer and thermal radiation in stagnation point flow of nanofluid past a stretching cylinder is tackled by Hayat et al. [6]. Nonlinear radiative MHD flow of Casson fluid subject to Cattaneo–Chirstov theory is discussed by Ramandevi et al. [7]. Stretched flow of Powell–Eyring nanoliquid with heat and mass flux conditions is addressed by Hayat et al. [8]. On the other side, the convective heat transport has also generated substantial attraction because of its excessive importance in the industrial and environmental technologies comprising gas turbines, nuclear plants, energy storage, rocket propulsion, photovoltaic panels and geothermal reservoirs. Referring to several engineering and industrial processes, the convective conditions are more practical including transpiration cooling, material drying, etc. Due to all these practical demands numerous researchers have inspected and reported convective surface condition via various aspects (see refs. [9–15]).

The analysis of dynamics of allosterically conducting liquid, i.e. magnetohydrodynamics is standout amongst the most noteworthy region of research since different engineering issues rely on it. Its importance is widely expressed in various aspects like metallurgy and metal working, pumps, droplet filter pumps, boundary layer control, bearings and MHD generators, in nuclear reactors, plasma investigation and geothermal energy extraction and polymer industry, in astrophysics and geophysics. Due to its wide applications many scientists carried out MHD flows in various physical phenomenons. Ellahi et al. [16] presented numerical study for MHD flow and heat transfer with nonlinear slip. Sheikholeslami et al. [17] reported the consequences of MHD flow of Cu–water nanofluid. Zhang et al. [18] examined chemical reaction in magnetohydrodynamic nanofluids flow with variable surface heat flux in porous media. MHD Oldroyed-B nanofluid flow over a radiative surface was explored by Shehzad et al. [19]. Hayat et al. [20] inspected flow of Sisko nanoliquid with magnetic aspects. Recently Hayat et al. [21] investigated MHD flow of Powell–Eyring nanoliquid with variable thickness. Some other studies about MHD flow can be seen via refs. [22–29].

Researchers and engineers are still interested to inspect the fluid flow when chemical reaction is present. Some general applications of chemical reactions including the formation and dispersion of fog, hydrometallurgical industry, ceramics and polymer production, energy supply in a wet cooling tower, water and air pollutions, damage of crops due to freezing, atmospheric flows, electric power generation and forbears insulation. No doubt reactions are of two types namely heterogeneous and homogeneous. Homogeneous reaction is occurring in the fluid while heterogeneous reaction is carried out on some catalyst surface. The influence of homogeneous–heterogeneous reactions in the stagnation-point layer fluid was reported by Chaudhary and Marken [30]. He intended various diffusivities of the reactants and autocatalyst. Bachok et al. [31] explored the homogeneous–heterogeneous effect in stagnation-point stretched flow. Rashidi et al. [32] reported the effect of mixed convection and chemical reactions through horizontal surface. The stretched flow of Maxwell fluid with homogeneous–heterogeneous reactions is examined by Hayat et al. [33]. Khan and Pop [34] put forward such effects on the flow of viscoelastic liquid over a stretching sheet. Hayat et al. [35] investigated the consequences of homogeneous–heterogeneous reactions in Jeffrey fluid.

Very less data are accessible in the literature about the fluid model suggested by Sisko [36]. Some significant attempts about Sisko can be consulted in the Refs. [37–41]. It should be pointed out that earlier investigators have not focused on homogeneous and heterogeneous reactions in flow of Sisko fluid. Thus our basic theme of present attempt is to fill such gaps. Especially the novelty of the current article is through the following aspects. Firstly to consider Sisko fluid model with effects of magnetohydrodynamic. Secondly to utilize convective heat transfer in the flow by stretched surface. Thirdly to carry out analysis in the presence of homogeneous and heterogeneous reactions. Fourth to develop numerical solutions via ND solve Shooting technique. The impact of distinct embedded variables on velocity, temperature and concentration are made and scrutinize graphically. Surface drag coefficients and mass transfer rate at the surface are also studied numerically. Further comparative study is provided which confirms the surety of our present attempt.

2 Formulation

Here we intend to inspect steady 3D incompressible flow of Sisko fluid. Stretched surface at $z = 0$ is responsible for the fluid flow. The surface stretching velocities along x- and y-directions are denoted by $U_w = cx$ and $V_w = dy$, respectively (where c and d are positive dimensional constants). Magnetic field of strength B_0 is utilized (see Fig. 1). Consequences of induced magnetic and electric fields are neglected. Heat transport characteristics incorporate the convective condition. Let T_∞ be ambient fluid temperature and T_f the hot liquid temperature which heated the bottom surface via convection. We assume a simple model of heterogeneous–homogeneous reaction:

$$A_1 + 2A_2 \rightarrow 3A_2, \text{ rate} = k_c a_1 b_1^2, \tag{1}$$

where the catalyst surface heterogeneous reaction is

$$A_1 \rightarrow A_2, \text{ rate} = k_s a_1. \tag{2}$$

Here the chemical species A_1 and A_2 have concentrations a_1 and b_1 respectively, while k_c and k_s are rate constants. Also both these reactions are isothermal. The resulting expressions after utilizing the boundary layer concept are:

$$\frac{\partial u}{\partial x} + \frac{\partial v}{\partial y} + \frac{\partial w}{\partial z} = 0, \tag{3}$$

$$\rho\left(u\frac{\partial u}{\partial x} + v\frac{\partial u}{\partial y} + w\frac{\partial u}{\partial z}\right) = a\frac{\partial^2 u}{\partial z^2} - b\frac{\partial}{\partial z}\left(-\frac{\partial u}{\partial z}\right)^n - \sigma B_0^2 u, \tag{4}$$

$$\rho\left(u\frac{\partial v}{\partial x} + v\frac{\partial v}{\partial y} + w\frac{\partial v}{\partial z}\right) = a\frac{\partial^2 v}{\partial z^2} + b\frac{\partial}{\partial z}\left(-\frac{\partial u}{\partial z}\right)^{n-1}\frac{\partial v}{\partial z} - \sigma B_0^2 v, \tag{5}$$

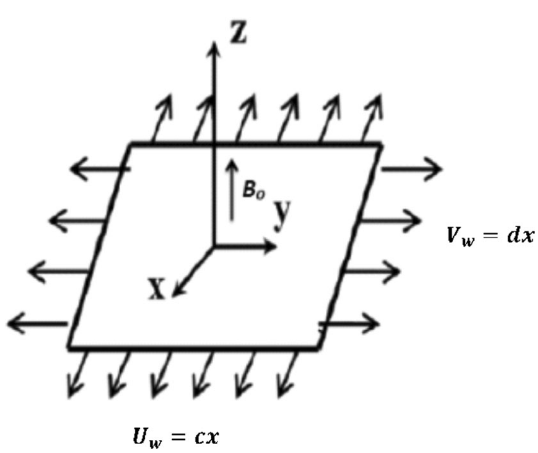

Fig. 1 Flow configuration

$$u\frac{\partial T}{\partial x} + v\frac{\partial T}{\partial y} + w\frac{\partial T}{\partial z} = \alpha_m \frac{\partial^2 T}{\partial y^2}, \tag{6}$$

$$u\frac{\partial a_1}{\partial x} + v\frac{\partial a_1}{\partial y} + w\frac{\partial a_1}{\partial z} = D_A\frac{\partial^2 a_1}{\partial z^2} - k_c a_1 b_1^2, \tag{7}$$

$$u\frac{\partial b_1}{\partial x} + v\frac{\partial b_1}{\partial y} + w\frac{\partial b_1}{\partial z} = D_B\frac{\partial^2 b_1}{\partial z^2} + k_c a_1 b_1^2. \tag{8}$$

The relevant conditions are

$$\left.\begin{array}{c} u = U_w = cx,\ v = V_w = dy,\ w = 0,\ -k\frac{\partial T}{\partial z} = h_f(T_f - T), \\ D_A\frac{\partial a_1}{\partial z} = k_s a_1,\ D_B\frac{\partial b_1}{\partial z} = -k_s a_1 \text{ at } z = 0, \end{array}\right\} \tag{9}$$

$$u \rightarrow 0,\ v \rightarrow 0,\ T \rightarrow T_\infty,\ a_1 \rightarrow a_0\, b_1 \rightarrow 0 \text{ when } z \rightarrow \infty. \tag{10}$$

Here the respective components of velocity in the (x, y, z) directions are designated by (u, v, w), ρ the density of liquid, D_A and D_B the respective diffusion species coefficients of A_1 and A_2 and a_0 the positive dimensionless constant, T the surface fluid temperature and $\alpha_m = \frac{k}{\rho c_p}$ the thermal diffusivity. Here a and b denote the material parameters of Sisko materials and $n > 0$ characterizes the non-Newtonian features of fluid. Further note that for $n = 1$, $a = 0$ and $b = \mu$ or $a = \mu$ and $b = 0$ the fluid is viscous. For $n > 1$ the behavior is dilatant (shear thickening) and $0 < n < 1$ the situation corresponds to pseudoplastic (shear-thinning). Make use of the following transformations [33, 41]:

$$\left.\begin{array}{c} u = cxf'(\xi),\ v = dg'(\xi),\ w = -c\left(\frac{c^{n-2}}{\rho/b}\right)^{1/(n+1)}\left(\frac{2n}{n+1}f + \frac{1-n}{n+1}\xi f' + g\right)x^{\frac{n-1}{n+1}}, \\ \theta(\xi) = \frac{T-T_\infty}{T_f-T_\infty},\ a_1 = a_0\phi(\xi),\ b_1 = a_0 h(\xi),\ \xi = z\left(\frac{c^{2-n}}{\rho/b}\right)^{1/n+1} x^{\frac{1-n}{1+n}}. \end{array}\right\} \tag{11}$$

Expression (3) is trivially verified and Eqs. (4)–(10) lead to:

$$\beta f''' + n(-f'')^{n-1}f''' + \left(\frac{2n}{n+1}\right)ff'' - (f')^2 + gf'' - M^2 f' = 0, \tag{12}$$

$$\beta g''' + (-f'')^{n-1}g''' - (n-1)g''f'''(-f'')^{n-2} + \left(\frac{2n}{n+1}\right)fg'' - (g')^2 + gg'' - M^2 g' = 0, \tag{13}$$

$$\theta'' + \Pr\left(\frac{2n}{n+1}\right)\theta' f + Prg\theta' = 0, \tag{14}$$

$$\frac{1}{Sc}\phi'' + \left(\frac{2n}{n+1}\right)f\phi' + g\phi' - k_1\phi h^2 = 0, \tag{15}$$

$$\frac{\delta_1}{Sc}h'' + \left(\frac{2n}{n+1}\right)fh' + gh' + k_1\phi h^2 = 0, \tag{16}$$

$$\left.\begin{array}{c} f = 0,\ g = 0,\ f' = 1,\ g' = \alpha,\ \theta' = -\gamma(1-\theta),\ \phi' = k_2\phi,\ \delta_1 h' = -k_2\phi \text{ at } \xi = 0, \\ f' \to 0,\ g' \to 0,\ \theta \to 0,\ \phi \to 1,\ h \to 0 \text{ when } \xi \to \infty. \end{array}\right\}. \tag{17}$$

Here β signifies the Sisko fluid material parameter, Re_a and Re_b show the local Reynolds numbers, M indicates the magnetic parameter, α designates the ratio parameter, k_1 signifies the measure of strength of homogeneous reaction, Pr denotes Prandtl number, k_2 shows measure of strength of heterogeneous reaction, Sc designates Schmidt number, δ_1 represents the diffusion coefficient ratio, γ the Biot number due to temperature and prime indicates derivative via ξ. These dimensionless quantities are expressed as follows:

$$\left.\begin{array}{c} \beta = \frac{Re_b^{\frac{2}{n+1}}}{Re_a},\ Re_a = \frac{\rho x U_w}{a},\ Re_b = \frac{\rho x^n U_w^{2-n}}{b},\ M^2 = \frac{\sigma B_0^2}{\rho c},\ \alpha = \frac{d}{c}, \\ k_1 = \frac{k_c a_0^2}{c},\ k_2 = \frac{k_s c x}{D_A z} Re_b^{\frac{-1}{(n+1)}},\ \gamma = \frac{h_f}{k} x Re_b^{\frac{-1}{(n+1)}}, \\ \Pr = \frac{Re_a Re_b^{\frac{-2}{n+1}}}{ak/c},\ Sc = \frac{D_A}{U_w x} Re_b^{\frac{2}{n+1}},\ \delta_1 = \frac{D_B}{D_A}. \end{array}\right\} \tag{18}$$

Note that for $\alpha = 1$ and $\alpha = 0$, the axisymmetric and two-dimensional flows are, respectively, reduced. The similarity solutions are possible only in the case $n = 1$ (for viscous fluid). In this situation, the parameters $\beta = 0$ and γ do not depend upon x, i.e. γ is constant. With these view points, our intention now is to develop local similar solutions since the parameters in present analysis depends on an independent variable x (for details one can see the studies [42–44]). Comparable size is presumed for the coefficients of diffusion of chemical species A_1 and A_2. This fact provides us to establish further supposition that the diffusion coefficients D_A and D_B are same, i.e. $\delta_1 = 1$ and thus [45–47]

$$\phi(\xi) + h(\xi) = 1.$$

Equations (15) and (16) yield

$$\frac{1}{Sc}\phi'' + \left(\frac{2n}{n+1}\right)f\phi' + g\phi' - k_1\phi(1-\phi)^2 = 0, \tag{19}$$

with the relevant conditions

$$\phi'(0) = k_2\phi(0),\ \phi(\infty) \to 1. \tag{20}$$

Surface drag coefficients along x- and y-directions are

$$\left.\begin{array}{r} Re_b^{\frac{1}{(n+1)}} C_{fx} = \beta f''(0) + (f''(0))^n, \\ Re_b^{\frac{1}{(n+1)}} C_{fy} = \frac{V_w}{U_w}(\beta g''(0) f(0) + (-f''(0))^{n-1} g''(0)). \end{array}\right\} \tag{21}$$

Expressions for local Nusselt number can be written as:

$$Re_b^{-1/(n+1)} Nu_x = -\theta'(0), \tag{22}$$

where $Re_a = \frac{\rho_f x U_w}{a}$ and $Re_b = \frac{\rho_f x^n U_w^{2-n}}{b}$ elucidate the local Reynolds numbers.

3 Method for solution

The considered problem is modeled through boundary layer assumptions. To compute the numerical solutions of Eqs. (12)–(14) and (20) with imposed boundary conditions stated in Eqs. (17) and (21), we utilized the ND solve Shooting technique via Mathematica. We also numerically executed the characteristics of surface drag coefficients and local Nusselt number for various emerging variables.

4 Result and discussion

Feature of numerous pertinent variables like magnetic parameter (M), Prandtl number (Pr), Biot number due to temperature (γ), ratio parameter (α), strength of homogeneous variable (k_1), Schmidt number (Sc), power law index (n) and strength of heterogeneous variable (k_2) on temperature $\theta(\xi)$ and concentration $\phi(\xi)$ are declared graphically in this portion. For such analysis Figs. 2, 3, 4, 5, 6, 7, 8, 9, 10, 11, 12 and 13 have been interpreted. Temperature profile against magnetic parameter M is demonstrated in

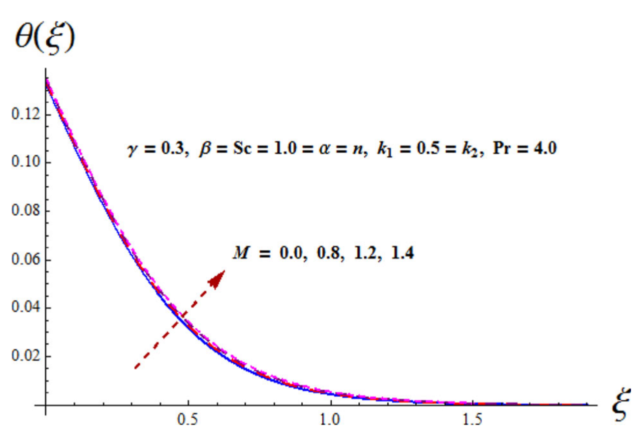

Fig. 2 Variation of $\theta(\xi)$ via M

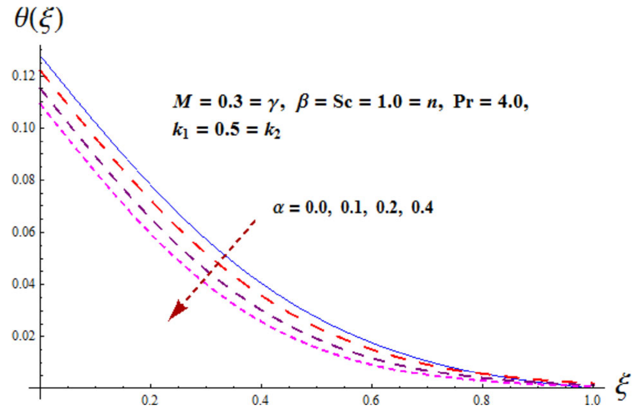

Fig. 3 Variation of $\theta(\xi)$ via α

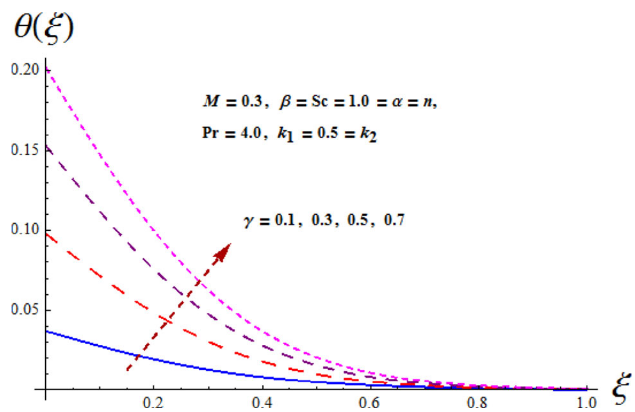

Fig. 4 Variation of $\theta(\xi)$ via γ

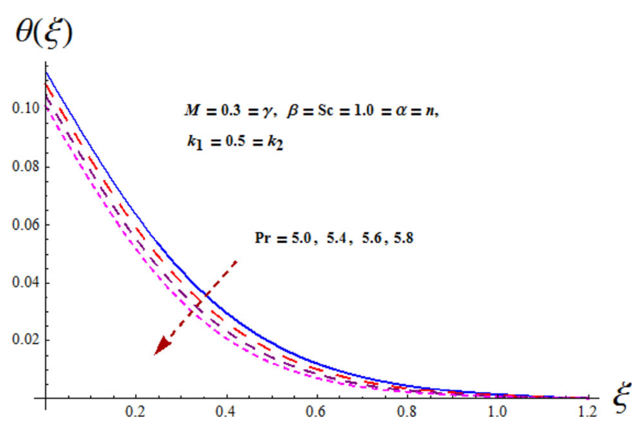

Fig. 5 Variation of $\theta(\xi)$ via Pr

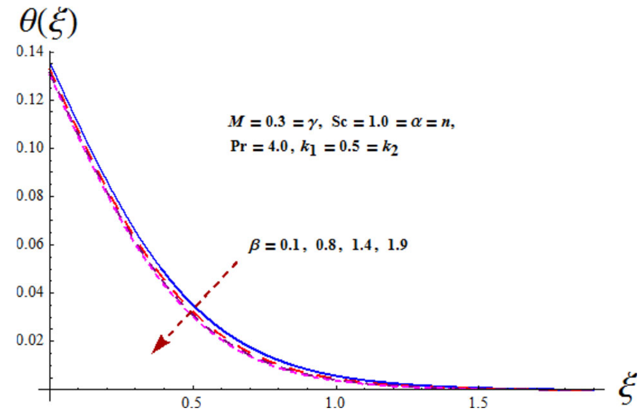

Fig. 6 Variation of $\theta(\xi)$ via β

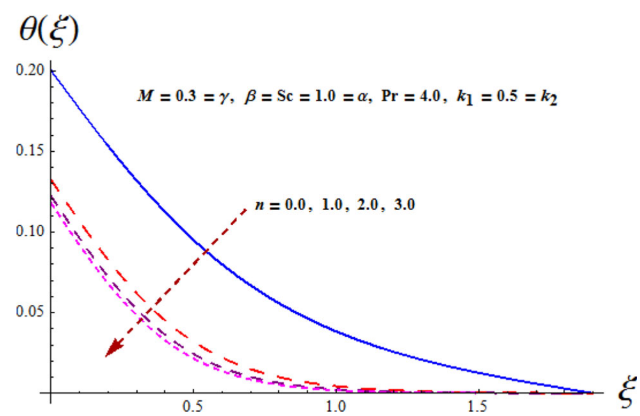

Fig. 7 Variation of $\theta(\xi)$ via n

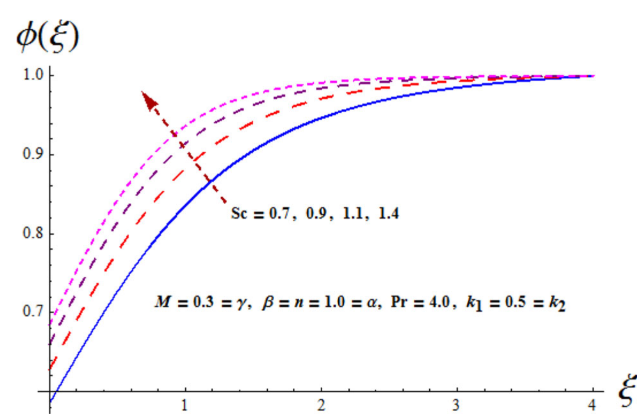

Fig. 8 Variation of $\phi(\xi)$ via Sc

Fig. 2. Here temperature field $\theta(\xi)$ is upgraded for higher M. This rise in temperature is due to heat generated by resistive force caused by magnetic field. Figure 3 is displayed to confess the significance of α on temperature $\theta(\xi)$. It is observed that liquid temperature decays with an increment in ratio parameter. Variation of Biot number γ on temperature distribution is depicted in Fig. 4. It is revealed that an enhancement in γ increases the temperature field. When γ is enhanced the convection resistance of side hot plate decreases and ultimately it rises $\theta(\xi)$. Feature of Pr on temperature field is presented in Fig. 5. Here we found that fluid temperature decreases with the increase in Pr. Since thermal diffusivity decreases for higher Pr so temperature diminishes. Characteristics of material parameter β on $\theta(\xi)$ is shown in Fig. 6. It is found that temperature profile diminishes via β. Also it is

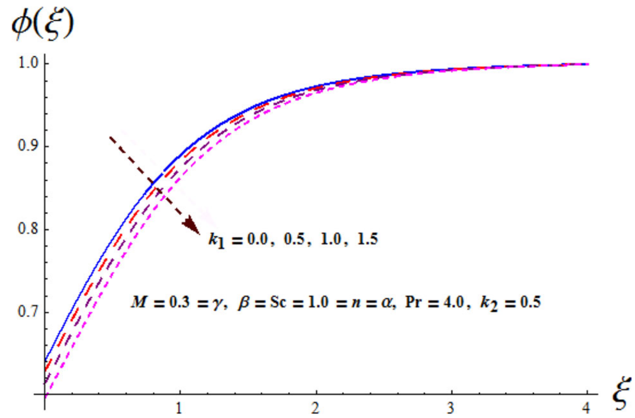

Fig. 9 Variation of $\phi(\xi)$ via k_1

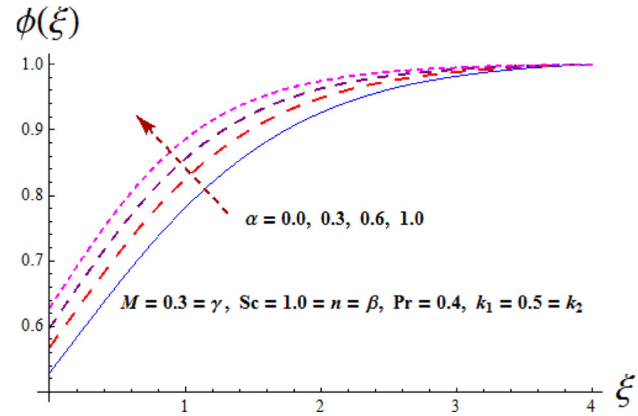

Fig. 12 Variation of $\phi(\xi)$ via α

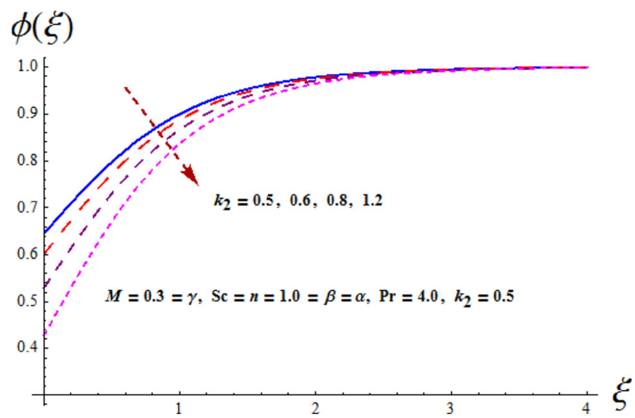

Fig. 10 Variation of $\phi(\xi)$ via k_2

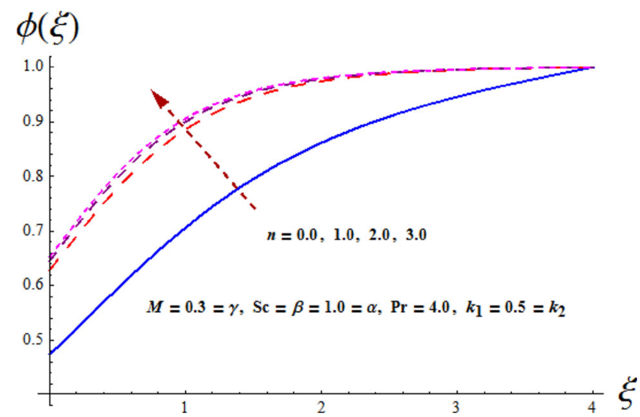

Fig. 13 Variation of $\phi(\xi)$ via n

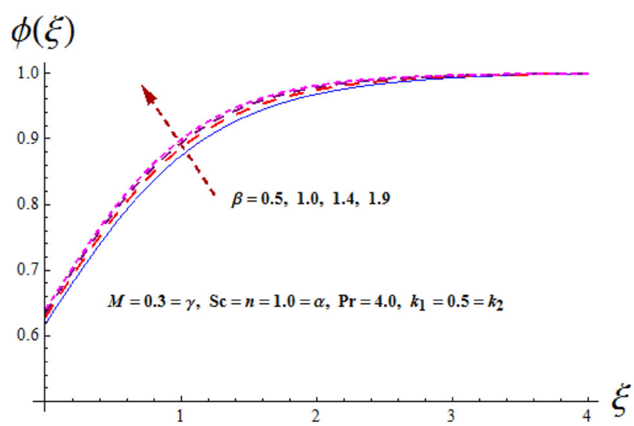

Fig. 11 Variation of $\phi(\xi)$ via β

interesting to mention that ($\beta = 0$ and $n = 1$) correspond to Newtonian fluid while ($\beta = 0$ and $n \neq 1$) shows the power-law fluid situation. In physical sense Sisko material parameter is ratio of higher shear rate viscosity to consistency index. Enhancement in Sisko fluid parameter corresponds to low consistency index (viscosity of fluid) at high shear rate and thus temperature is decreased. An increment in n decays the temperature field $\theta(\xi)$ (see Fig. 7). Higher viscosity is associated with larger values of n which implies that temperature field is reduced. Further it is concluded that influence of β on $\theta(\xi)$ dominates for shear thinning when compared with other value of n. Impact of Sc on concentration profile is declared in Fig. 8. As Sc is equal to viscous diffusion divided by molecular diffusion rate, an increment in Sc diminishes the molecular diffusion rate and consequently there is an increase in fluid concentration. The effect of homogeneous reaction parameter k_1 on concentration field $\phi(\xi)$ is drawn in Fig. 9. In fact more reactants are consumed when k_1 is enhanced. This leads to decrease in the concentration distribution $\phi(\xi)$. Similar phenomenon is observed for k_2 (see Fig. 10). Figure 11 illustrates variation of β on concentration distribution. Here higher concentration profile is associated with varying β. In fact increment in Sisko material parameter leads to higher ratio of higher shear rate viscosity. It raises the concentration and its corresponding boundary layer thickness. The impact of α on concentration field is portrayed in Fig. 12. It is depicted that $\phi(\xi)$ has increasing behavior via α. Figure 13 elucidates feature of n on $\phi(\xi)$.

Table 1 Numerical data of surface drag coefficients via various pertinent variables

Parameter constant values	Parameters	Values	$-\mathrm{Re}_a^{\frac{1}{(n+1)}}C_{fx}$	$-\mathrm{Re}_b^{\frac{1}{(n+1)}}C_{fy}$
$\gamma = 0.3,\ \alpha = \beta = 1.0 = n = Sc, k_1, = 0.5 = k_2, \mathrm{Pr} = 4.0$	M	0.0	1.6292	1.8146
		0.3	1.6843	1.8421
		0.6	1.8404	1.92,022
$\gamma = 0.3 = M,\ \alpha = 1.0 = n = Sc, k_1, = 0.5 = k_2, \mathrm{Pr} = 4.0$	β	0.0	1.1921	2.1921
		0.5	1.4577	1.9718
		1.0	1.6843	1.8421
$\gamma = 0.3 = M,\ \beta = 1.0 = n = Sc, k_1, = 0.5 = k_2, \mathrm{Pr} = 4.0$	α	0.0	1.4973	1.7486
		0.5	1.4941	1.7971
		1.2	1.7188	1.8594
$\gamma = 0.3 = M,\ \beta = \alpha = 1.0 = Sc, k_1, = 0.5 = k_2, \mathrm{Pr} = 4.0$	n	1.0	1.9803	1.8421
		2.0	1.9803	1.9620
		3.0	2.2154	2.1636

Table 2 Comparison of skin friction coefficients for different values of α when $A = 0.0 = M$ and $n = 1.0$

	$-f''(0)$		$-g''(0)$	
α	Present results	HAM [35]	Present results	HAM [35]
0.0	1.00000	1.00000	0.00000	0.00000
0.3	1.055234	1.057955	0.234632	0.243359
0.5	1.090504	1.093095	0.458035	0.465205
0.8	1.149069	1.142489	0.859627	0.866683
1.0	1.172897	1.173722	1.698852	1.173722

Clearly $\phi(\xi)$ is increasing function of n. When we increase the values of n, fluid viscosity increases which consequently raise the concentration layer thickness. The numerical data of surface drag coefficients associated with various sundry variables M, n, α, and β (when $Sc = 1.0$, $k_1 = 0.5 = k_2$ and $Pr = 4.0$) are declared in Table 1. It is reported that surface drag coefficients in both x- and y-directions are enhanced via M, n, α and β. Comparison of some numerical values of skin frictions in present analysis with that of Hayat et al. [35] are captured via Table 2. All the outcomes are found in good agreement. Table 3 is constructed to analyze the variation of surface heat transfer rate $(Re_b^{-1/(n+1)}Nu_x)$ for numerous values of involved variables M, γ, α, β, Sc and Pr when $n = 1.0$ and $k_1 = 0.5 = k_2$. It is inspected that rising values of γ, α, β and Pr result local Nusselt number enhancement. However, reverse behavior is analyzed for larger M.

Table 3 Numerical data of local Nusselt number $-\theta'(0)$ via M, γ, α, β, Pr and Sc when keeping k_1, k_2 and n fixed

Parameter (constant values)	Parameters	Values	$-\theta'(0)$
$\gamma = 0.3,\ \alpha = \beta = 1.0 = n = Sc, k_1, = 0.5 = k_2, \mathrm{Pr} = 4.0$	M	0.0	0.26167
		0.5	0.26148
		1.2	0.26103
$\gamma = 0.3 = M,\ \alpha = 1.0 = n = Sc, k_1, = 0.5 = k_2, \mathrm{Pr} = 4.0$	β	0.0	0.26023
		0.6	0.26124
		1.3	0.26182
$\gamma = 0.3 = M,\ \beta = 1.0 = n = Sc, k_1, = 0.5 = k_2, \mathrm{Pr} = 4.0$	α	0.0	0.24807
		0.5	0.25513
		1.2	0.26162
$M = 0.3 = \gamma,\ \beta = \alpha = 1.0 = n, k_1, = 0.5 = k_2, \mathrm{Pr} = 4.0$	γ	0.1	0.09533
		0.5	0.46389
		1.0	0.67160
$M = 0.3 = \gamma,\ \beta = \alpha = 1.0 = Sc = n, k_1, = 0.5 = k_2$	Pr	0.9	0.22071
		1.4	0.23603
		1.9	0.24626
$M = 0.3 = \gamma,\ \beta = \alpha = 1.0 = n, k_1, = 0.5 = k_2, \mathrm{Pr} = 4.0$	Sc	0.8	0.26162
		1.	0.26162
		1.4	0.26162

5 Concluding remarks

Particular points of present study are:

- An increment in M demonstrates decay in fluid temperature.
- Temperature $\theta(\xi)$ is enhanced via γ and α.
- Homogeneous and heterogeneous reactions have similar effect on concentration field.
- Increasing values of n show opposite behavior for the temperature and concentration fields.
- Surface drag coefficients is enhanced via M and α.
- Magnitude of surface heat transfer rate is more for larger values of α, β, γ and Pr.

References

1. Crane LJ (1970) Flow past a stretching plate. J Appl Math Phys (ZAMP) 21:645–647
2. Cortell R (2008) Effects of viscous dissipation and radiation on the thermal boundary layer over a nonlinearly stretching sheet. Phys Lett A 372:631–636
3. Ibrahim W, Shankar B, Nandeppanavar MM (2013) MHD stagnation point flow and heat transfer due to nanofluid towards a stretching sheet. Int J Heat Mass Transfer 65:1–9
4. Mustafa M, Mushtaq A, Hayat T, Alsaedi A (2015) Radiation effects in three-dimensional flow over a bi-directional exponentially stretching sheet. J Taiwan Inst Chem Eng 47:43–49
5. Hsiao KL (2016) Stagnation electrical MHD nanofluid mixed convection with slip boundary on a stretching sheet. Appl Therm Eng 98:850–861
6. Hayat T, Ijaz Khan M, Waqas M, Alsaedi A, Farooq M (2017) Numerical simulation for melting heat transfer and radiation effects in stagnation point flow of carbon–water nanofluid. Comput Methods Appl Mech Eng 315:1011–1024
7. Ramandevi B, Reddy JVR, Sugunamma V, Sandeep N (2017) Combined influence of viscous dissipation and non-uniform heat source/sink on MHD non-Newtonian fluid flow with Cattaneo–Christov heat flux. Alex Eng J. https://doi.org/10.1016/j.aej.2017.01.026
8. Hayat T, Ullah I, Muhammad T, Alsaedi A, Shehzad SA (2016) Three-dimensional flow of Powell–Eyring nanofluid with heat and mass flux boundary conditions. Chin Phys B 25:074701
9. Makinde OD, Aziz A (2011) Boundary layer flow of a nanofluid past a stretching sheet with a convective boundary condition. Int J Therm Sci 50:1326–1332
10. Hayat T, Muhammad K, Farooq M, Alsaed A (2016) Unsteady squeezing flow of carbon nanotubes with convective boundary conditions. PLoS One 11:e0152923
11. Hayat T, Imtiaz M, Alsaedi A, Mansoor R (2014) MHD flow of nanofluids over an exponentially stretching sheet in a porous medium with convective boundary conditions. Chin Phys B 23:054701
12. Rosali H, Ishak A, Nazar R, Pop I (2016) Mixed convection boundary layer flow past a vertical cone embedded in a porous medium subjected to a convective boundary condition. Propuls Power Res 5:118–122
13. Hayat T, Ullah I, Muhammad T, Alsaedi A (2016) Magnetohydrodynamic (MHD) three-dimensional flow of second grade nanofluid by a convectively heated exponentially stretching surface. J Mol Liq 220:1004–1012
14. Hayat T, Ullah I, Muhammad T, Alsaedi A (2017) A revised model for stretched flow of third grade fluid subject to magneto nanoparticles and convective condition. J Mol Liq 230:608–615
15. Hayat T, Ullah I, Alsaedi A, Waqas M, Ahmad B (2017) Three-dimensional mixed convection flow of Sisko nanoliquid. Int J Mech Sci. https://doi.org/10.1016/j.ijmecsci.2017.07.037
16. Ellahi R, Hameed M (2012) Numerical analysis of steady flows with heat transfer MHD and nonlinear slip effects. Int J Numer Method Heat Fluid Flow 22:24–38
17. Sheikholeslami M, Bandpy MG, Ganji DD, Soleimani S (2014) Natural convection heat transfer in a cavity with sinusoidal wall filled with # water nanofluid in presence of magnetic field. J Taiwan Inst Chem Eng 45:40–49
18. Zhang L, Zheng X Zhang, Chen G (2015) MHD flow and radiation heat transfer of nanofluids in porous media with variable surface heat flux and chemical reaction. Appl Math Mod 39:165–181
19. Shehzad SA, Abdullah Z, Alsaedi A, Abbasi FM, Hayat T, Alsaedi A (2016) Magnetic field effect in three-dimensional flow of an Oldroyed-B nanofluid over a radiative surface. J Magn Magn Mater 399:97–108
20. Hayat T, Muhammad T, Shehzad SA, Alsaedi A (2016) On three-dimensional boundary layer flow of Sisko nanofluid with magnetic field effects. Adv Powder Technol 27:504–512
21. Hayat T, Ullah I, Alsaedi A, Farooq M (2017) MHD flow of Powell–Eyring nanofluid over a non-linear stretching sheet with variable thickness. Results Phys 7:189–196
22. Ali ME, Sandeep N (2017) Cattaneo–Christov model for radiative heat transfer of magnetohydrodynamic Casson–ferrofluid: a numerical study. Results Phys 7:21–30
23. Ramzan M, Farooq M, Alsaedi A, Hayat T (2013) MHD three-dimensional flow of couple stress fluid with Newtonian heating. Eur Phys J Plus 128:49
24. Reddy JVR, Sugunamma V, Sandeep N (2016) Cross diffusion effects on MHD flow over three different geometries with Cattaneo–Christov heat flux. J Mol Liq 223:1234–1241
25. Hayat T, Ullah I, Alsaedi A, Ahmad B (2017) Modeling tangent hyperbolic nanoliquid flow with heat and mass flux conditions. Eur Phys J Plus 132:112
26. Makinde OD, Sandeep N, Animasaun IL (2017) Numerical exploration of Cattaneo–Christov heat lux and mass transfer in magnetohydrodynamic flow over various geometries. Def Diff Forum 374:67–82
27. Hayat T, Ullah I, Ahmed B, Alsaedi A (2017) MHD mixed convection flow of third grade liquid subject to non-linear thermal radiation and convective condition. Results Phys. https://doi.org/10.1016/j.rinp.2017.07.045
28. Kumar MS, Sandeep N, Kumar BR, Prakash J (2017) Effect of Cattaneo–Christov heat flux on nonlinear radiative mhd flow of Casson fluid induced by a semi infinite stretching surface. Front Heat Mass Transfer (FHMT) 8:8
29. Hayat T, Ullah I, Ahmad B, Alsaedi A (2017) Radiative flow of Carreau liquid in presence of Newtonian heating and chemical reaction. Results Phys 7:715–722
30. Chaudhary MA, Merkin JH (1995) A simple isothermal model for homogeneous–heterogeneous reactions in boundary-layer flow. I equal diffusivities. Fluid Dyn Res 16:311–333
31. Bachok N, Ishak A, Pop I (2011) On the stagnation point flow towards a stretching sheet with homogeneous–heterogeneous reactions effects. Commun Nonlinear Sci Numer Simul 16:4296–4302
32. Rashidi MM, Rahimzadeh N, Ferdows M, Jashim Uddin MD, Anwar Beg O (2012) Group theory and differential transformed analysis of mixed convection heat and mass transfer from a

horizontal surface with chemical reaction effects. Chem Eng Commun 199:1012–1043
33. Hayat T, Imtiaz M, Almezal S (2015) Modeling and analysis for three-dimensional flow with homogeneous–heterogeneous reactions. AIP Adv 5:107209
34. Khan WA, Pop I (2015) Effects of homogeneous–heterogeneous reactions on the viscoelastic fluid towards a stretching sheet. ASME J Heat Transfer 134:1–5
35. Hayat T, Qayyum S, Imtiaz M, Alsaedi A (2016) Impact of Cattaneo–Christov heat flux in Jeffrey fluid flow with homogeneous–heterogeneous reactions. PLoS One 11:e0148662
36. Sisko AW (1958) The flow of lubricating greases. Ind Eng Chem 50:1789–1792
37. Abelman S, Hayat T, Momoniat E (2009) On the Rayleigh problem for a Sisko fluid in a rotating frame. Appl Math Comput 215:2515–2520
38. Hayat T, Moitsheki RJ, Abelman S (2010) Stokes' first problem for Sisko fluid over a porous wall. Appl Math Comput 217:622–628
39. Munir A, Shahzad A, Khan M (2015) Convective flow of Sisko fluid over a bidirectional stretching surface. PLoS One 10:e0130342
40. Khan M, Malik R (2016) Forced convective heat transfer to Sisko nanofluid past a stretching cylinder in the presence of variable thermal conductivity. J Mol Liq 218:1–7
41. Hayat T, Muhammad T, Ahmad B, Shehzad SA (2016) Impact of magnetic field in three-dimensional flow of Sisko nanofluid with convective condition. J Magn Magn Mater 413:1–8
42. Rahman MM (2011) Locally similar solutions for hydromagnetic and thermal slip flow boundary layers over a flat plate with variable fluid properties and convective surface boundary condition. Meccanica 46:1127–1143
43. Sanjayanand E, Khan SK (2006) On heat and mass transfer in a viscoelastic boundary layer flow over an exponentially stretching sheet. Int J Therm Sci 45:819–828
44. Subhashini SV, Samuel N, Pop I (2011) Double-diffusive convection from a permeable vertical surface under convective boundary condition. Int Commun Heat Mass Transfer 38:1183–1188
45. Kameswaran PK, Shaw S, Sibanda P, Murthy PVSN (2013) Homogeneous–heterogeneous reactions in a nanofluid flow due to a porous stretching sheet. Int J Heat Mass Transfer 57:465–472
46. Hayat T, Farooq M, Alsaedi A (2015) Homogeneous–heterogeneous reactions in the stagnation point flow of carbon nanotubes with Newtonian heating. AIP Adv 5:027130
47. Hayat T, Kiran A, Imtiaz M, Alsaedi A (2017) Effect of homogeneous–heterogeneous reactions in stagnation point flow of third grade fluid past a variable thickness stretching sheet. Neural Comput Appl. https://doi.org/10.1007/s00521-017-2913-z